Monolithically Integrated Resonant Cavity Enhanced Type-II Superlattice Detectors

Leland Nordin, Abhilasha Kamboj, Priyanka Petluru, Narae Yoon, Daniel Wasserman

University of Texas Austin, Department of Electrical and Computer Engineering, Austin, TX 78758

nordin@utexas.edu

Abstract: We demonstrate all-epitaxial resonant cavity-enhanced type-II superlattice detectors (T2SL). Our structures show peak quantum efficiencies of 43-59%, which is a 4.0-6.6x enhancement compared to our control structures and greater than state-of-the-art long-wavelength infrared T2SL detectors.

1. Introduction

The mid-infrared (mid-IR) wavelength range is of vital importance for a range of sensing, security and defense, and fundamental science applications. While mid-IR source development has been accelerated by the demonstration and subsequent commercialization of the quantum cascade laser, the state-of-the-art mid-IR detector (HgCdTe) has remained fixed for the past several decades. More recently, the type II superlattice detector has been proposed as an alternative to HgCdTe for the infrared [1]. Mid-IR detector structures using T2SL materials allow for design-dependent, wavelength flexible operation and are suggested to be able to achieve improved performance over state-of-the-art mid-IR detectors. However, typical T2SL detectors have weak absorption compared to bulk semiconductors at the same wavelengths, and thus require thick absorber layers, which increases the materials cost and time of detector growth, as well as decreases tolerances for strain accumulation due to lattice mismatch. In addition, because of the limited diffusion length of photoexcited carriers, the probability of collection decreases as the absorption event moves farther from the surface of the detector. There is thus significant motivation to design either detector materials, or detector architectures, which are capable of strong absorption in thin ($< 2\,\mu m$) absorber regions [2–5]. In this work we leverage the high reflectance and tunability of highly doped semiconductors to realize monolithically integrated thin resonant cavity-enhanced (RCE) long-wavelength infrared (LWIR) detectors.

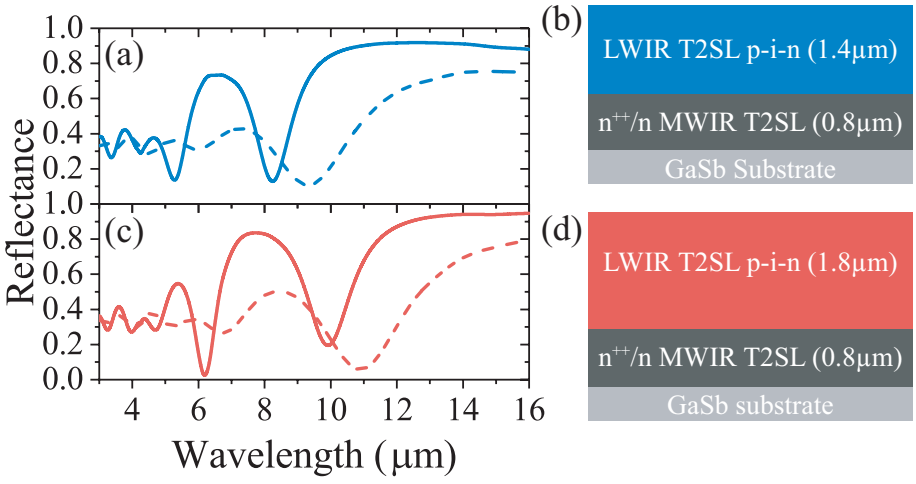

Fig. 1. (a) Reflectance spectra from the 8 μm RCE detector (solid) and control detector (dashed) and (b) sample structure of the 8 μm RCE/control detector. (c) Reflectance spectra from the 10 μm RCE detector (solid) and control detector (dashed) and (d) sample structure of the 10 μm RCE/control detector. Clear dips in reflectance are seen at 8 μm for the 1.4 μm thick detector and 10 μm for the 1.8 μm thick detector.

2. Results

Our structures are grown by molecular beam epitaxy on a GaSb substrate, the sample and control layer structures shown in Figure 1(b,d). To demonstrate the tunability of this system we grew two cavity thicknesses targeting a 8 µm and 10 µm cavity resonance. The highly doped material consists of a 800 nm thick silicon doped mid-wave infrared (Si:MWIR) InAs/InAsSb T2SL (n^{++}) layer grown lattice-matched to the GaSb substrate. For the control sample, we grow 800 nm of lightly doped (n) Si:MWIR InAs/InAsSb T2SL in place of the n^{++} MWIR T2SL layer. Following the MWIR T2SL growth a 1.4 µm (1.8 µm) thick InAs/InAsSb pin T2SL is grown, designed for a cutoff wavelength of 12 µm and a target absorption enhancement of $\lambda \sim 8$ µm (~ 10 µm). Figure 1(a,c) shows the experimental reflectance for both the 8 µm and 10 µm RCE detectors, and each detector's undoped counterpart. As one can see, there are clear dips in reflectance around 8 µm and 10 µm for each respective sample, suggesting the presence of an optical cavity.

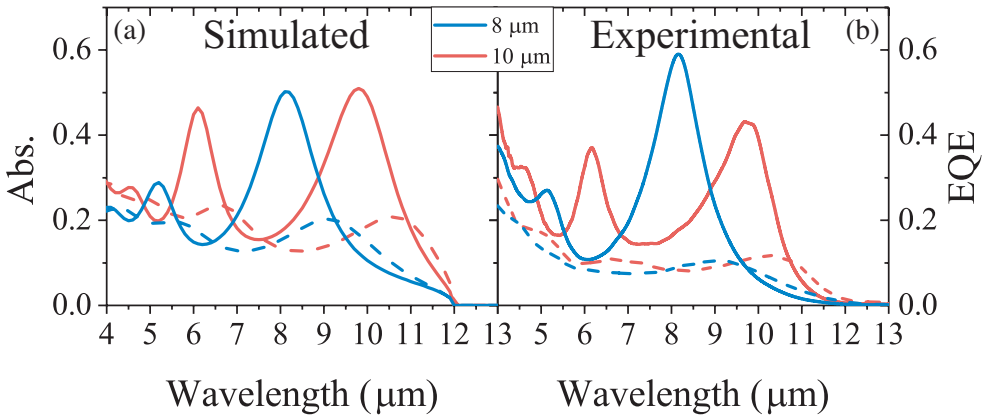

Fig. 2. (a) Simulated absorption for both the 8 µm and 10 µm enhanced and control devices. (b) EQE for both the 8 µm (blue) and 10 µm (red) enhanced detectors with their respective control's EQE plotted as dashed lines. On resonance, the 8 µm and 10 µm enhanced structures have approximately 59% and 43% EQE respectively.

Fabricated detectors are then mounted into a cryostat where spectral response and responsivity measurements are performed. Shown in Figure 2(a) is the modeled absorption for the as-grown optical stack; for these simulations the doped layer is modeled with a simple Drude model, and the T2SL absorption is modeled with a $\sqrt{E}$ dependence. Figure 2(b) presents the measured external quantum efficiency (EQE) of the 8 µm/10 µm enhanced and control structures. The spectral position of the enhancement feature corresponds to the design wavelength and the magnitude of the observed enhancement is $\sim 6.6\times$ in the 8 µm case and $\sim 4.0\times$ in the 10 µm case. For the 8µm structure the peak quantum efficiency is 59%, which is greater than state of the art T2SL work [6] and competitive with commercial MCT detectors.

3. Conclusion

We have demonstrated an all-epitaxial resonant cavity enhanced architecture which provides a $6.6\times$ ($4.0\times$) enhancement in EQE for the detectors designed for $\lambda = 8$ µm ($\lambda = 10$ µm) peak absorption. This enhancement amounts to a peak EQE of 59% (43%) in the 8 µm (10 µm) RCE detector, which is greater than the state-of-the-art for T2SL LWIR detectors. Additional improvements could be made to these detector structures by adding a grating to increase the EQE further or by implementing a nBn detector architecture in place of the p-i-n structure, dramatically reducing dark current.

LN, AK, PP, NY, and DW acknowledge support from Lockheed Martin. Additionally, DW and LN gratefully acknowledge support from the National Science Foundation (ECCS-1926187).

References

1. D. L. Smith et al. *J. Appl. Phys*, 62(6):2545, (1987).
2. S. Wang et al. *Appl. Phys. Lett.*, 112(9):091104, (2018).
3. M. Goldflam et al. *Appl. Phys. Lett.*, 109(25):251103, (2016).
4. V. Letka et al. *Opt. Express*, 27(17):23970, (2019).
5. J. Nolde et al. *Appl. Phys. Lett.*, 106(26):261109, (2015).
6. D. Ting et al., January 10 (2019). US Patent App. 15/530,294.